Novel Electrically Conductive Melamine-formaldehyde Nanocomposite Based on Graphite Nanosheets

Ahmed A. Abdala,[1,2] Claudia Pretschuh,[3] Clemens Schwarzinger,[3] Sunil Lonkar,[1] Sulafudin Vukusic[1]*

Summary: Conductive polymer composites based on carbon materials are widely used in commercial applications. Herein, electrically conductive melamine-formaldehyde (MF) resin was fabricated by incorporating various loadings of graphite nanosheets (GNS) via in-situ polymerization followed by crosslinking at 165 °C. The effect of GNS loading on the electrical conductivity, interfacial properties and thermal stability of the composites is discussed. SEM fractogram confirm the uniform dispersion and toughening of MF upon GNS reinforcement. The electrical percolation was achieved at about 0.9 vol.% loading of GNS suggesting an aspect ratio for GNS between 130 and 240 depending on the model used.

Keywords: electrical conductivity; graphite nanosheets; melamine-formaldehyde; nanocomposites; thermosets

Introduction

In the last few decades, polymer composites with electrically conductive fillers such as graphite, carbon black, or metal powder have been studied due to their functional applications in, for example, anti-static and corrosion resistant coatings and electromagnetic shielding. However, a relatively large filler quantity is required to achieve the targeted electrical conductivity and this high filler content is often associated with processing difficulties and degradation of the mechanical properties. Therefore, polymer composites with nanoscale conductive fillers have recently attracted considerable attention because a conductive network can be formed with very low filler content when a nanosize filler is homogeneously dispersed in the polymer matrix. Natural graphite, which is often used as conductive filler[1–4] exhibits high electrical conductivity of 10^4 S/cm at room temperature derived from the delocalized π bonds of sp^2 hybridized carbon atoms. Natural graphite consists of alternate graphene layers spaced by 3.4 bonded by weak van der Waals forces. Different methods are currently available for the separation/exfoliation of the atomic thick graphene sheets. Among these methods, thermal exfoliation of graphite oxide is suitable for mass production of thermally reduced graphene sheets. Upon oxidation of graphite, the interplanar spacing increases from 0.335 nm to approximately 0.789 nm[5] due to intercalation of water molecules. If graphite oxide is subjected to rapid thermal treatment, the intercalated molecules are evaporated and expanded graphite, also known as graphite nanosheets (GNS) consisting multilayer graphene are formed. During this exfoliation process the layer spacing is expanded and the initial volume of the compound is significantly increased few hundred times. The higher the exfoliation temperature, the larger the increase in the interlayer spacing and the exfoliation volume has also been

---

[1] Department of Chemical Engineering, The Petroleum Institute, Abu Dhabi, UAE
Fax: +971-2-607-5200; E-mail: aabdala@pi.ac.ae

[2] Department of Chemical Engineering and Petroleum Refining, Suez University, Suez, Egypt

[3] Institute for Chemical Technology of Organic Materials, Johannes Kepler University Linz, Altenbergerstrasse 69, Linz, Austria

observed.[6] The obtained GNS possesses a porous structure with different sizes and incoherent layers in nanometer scale and also called "nanoplatelete".

GNS can be mass-produced and applied to various fields such as gaskets, batteries, fire retardants and oil absorbing materials.[7] Due to its porous structure and surface functionality such GNS are suitable multifunctional filler for polymer nanocomposites. Therefore expanded graphite was widely used as conductive filler for thermoplastics and thermosets. Thermoplastics GNS nanocomposites with polyamide-6,[5] polymethyl methacrylate,[7–9] polypropylene,[10,11] polystyrene,[12,13] polystyrene acrylonitrile copolymer,[14] epoxy resins,[15,16] PPS,[17] polyaniline,[18] and polyesters[19] were reported. On the other hand, composites of thermosets su'ch as phenol formaldehyde resins with fillers like graphite powder,[1] carbon nanotubes,[20] or expanded graphite[21] were developed for production of electrically conductive cross-linked material. However, to the best of our knowledge the use of graphite based materials as a conductive filler in aminoplastic resins e.g. melamine formaldehyde (MF) has not been reported. MF is a water-based amino resin with excellent thermo-mechanical and coating properties, as well as appearance, and thus MF is extensively used in coating applications. These resins are commercially produced in large scale because of their applications in manufacturing of laminates, plywood and furniture, in varnishes and as moulding materials. Moreover, the processing characteristics of MF are favorable. The addition of conductive filler such as GNS can imaprt multifuntional properties, in particular electrical conductivity, to the MF which posses potential for various advanced applications.

In general, polymer composites filled with GNS are processed via either melt blending, solvent assisted mixing, or situ polymerization. In situ-polymerization is preferred for thermosets in order to improve the dispersion of the nanofiller into the polymer matrix, which can be enhanced by ultrasonic treatment to ensure the homogeneous dispersion of nanofillers. For example, GNS can be dispersed in polar solvents such as NMP, DMF, dichlorobenzene, nitromethane and THF.[22] With increasing the filler content most of the composites showed an improvement in electrical conductivity and some composites also shows enhancement in the thermal and the mechanical properties. Only a small loading of GNS were needed to reach the electrical percolation threshold, representing the insulator to conductor transition.[17–19]

In the present study, GNS are used as a conductive filler for the development of a conductive melamine formaldehyde composite. GNS were prepared by thermal exfoliation of graphite oxide. The structure and morphology of synthesized GNS were elucidated by X-ray diffraction (XRD) and scanning electron microscopy (SEM). The incorporation of GNS into the melamine formaldehyde resin was carried out by an in situ polymerization in tetrahydrofuran (THF). The effect of filler addition on the structure and thermal properties of final resin composites was studied by XRD, SEM, and thermogravimetric analysis (TGA). The effect of GNS loading on the electrical resistance is also discussed.

Experimental Part

Materials

Natural flake graphite (100 mesh, Sigma-Aldrich), potassium chlorate (Sigma-Aldrich), nitric acid (65%, Sigma-Aldrich), sulphuric acid (95–97%, Sigma-Aldrich), formaldehyde (35%, stabilized with 10% methanol, Riedel-de-Haën.) and tetrahydrofurane (Riedel-de-Haën) were used as received. Melamine was kindly supplied by AMI Agrolinz Melamine International GmbH.

Preparation of GNS

GNS was produced by a two-step process.[23] In the first step, graphite flakes (10 g) were oxidized with potassium chlorate (110 g) in a solution of nitric (90 ml) and sulfuric acid (180 ml) under magnetic stirring for 120 h. Nitrogen inertization with ice cooling was used to reduce the formation of chlorine dioxide gas which can occur during the addition of potassium chlorate. The reaction was stopped by adding water. The brownish slurry of the resulting graphite oxide was washed with hydrochloric acid (5%) then repeatedly with water to remove acidic traces and was then dried in air then in a vacuum at 40 °C. In the second step, the prepared graphite oxide was exfoliated through rapid heating to obtain GNS. The graphite oxide (700 mg) was put into a quartz tube of a tube furnace at 950 °C under nitrogen flow for 30 s. The expansion is detectable through increasing gas outcome and large volume increase.

Preparation of the Composite

The GNS inclusion into MF resin was accomplished by in situ polymerization. First, GNS was added during the methylolation reaction which represents the first step of the MF resin synthesis.[24] Since, GNS sheets do not homogeneously disperse in water; the synthesis was carried out in tetrahydrofurane. For improved curing, formaldehyde to melamine ratio of 1:3 was used. No curing reagent was used to avoid the influence of additives on the properties of the composite. Typically, melamine (100 g) with 0.1 to 3 wt.% GNS was dispersed in tetrahydrofurane (100 ml) by sonication. The suspension is heated to 65 °C and formaldehyde (188 ml of 30% aqueous solution) with pH adjusted to 8 using 1 M NaOH. After melamine is completely dissolved as indicated by the colour change from a white-grey suspension into a clear black solution, the reaction is carried out for additional 15 minutes. After synthesis, the produced black resin solution was either cured in a drying oven at a minimum temperature of 140 °C to obtain samples for SEM or the solvent was evaporated under reduced pressure and the solid resin is grounded and sieved. The obtained grey solid resin were then placed into a mould, cold pressed and then cured by hot pressing at 160 °C and 2 MPa for 5–10 minutes to prepare test specimens.

Composite Characterization

The crystalline structures of the synthesized graphite oxide and GNS was analysed by XRD (X'Pert Pro X-Ray diffractometer Philipps) using CuKα radiation. SEM (1540 XB Zeiss) was used to define the particle size and the structure of GNS and to confirm its uniform distribution into the melamine formaldehyde resins. In order to avoid charging, a static inhibitor was added to the MF resins during their synthesis and the cured resin samples were gold coated. The thermal stability of the GNS filled resins was tested by TGA (Shimadzu TGA 50) at 20 °C min^{-1} in a helium atmosphere. Surface resistance was measured using an 11-point DC surface resistance meter (PRS-801, Prostat). Each data point of electrical resistance was number averaged results from 5 measurements.

Results and Discussion

Characterization of GNS

The successful expansion process of graphite to GNS of graphite was primarily revealed by the following four characteristic observations: (i) a hundredfold volume expansion of graphite oxide after thermal treatment, (ii) high surface area (iii) elimination of all XRD diffraction peaks associated with parent graphite and (iv) formation of a porous worm-like nano structure existing of nanosheets. It is observed that the graphite was expanded by 100 to 150 times and the obtained GNS exhibits a specific volume of 200 to 300 ml g^{-1} and a specific surface area of 550 to 600 $m^2 g^{-1}$ (measured by the BET adsorption method). These values for exfoliation are comparable with other studies which describe a volume expansion ratio of 200 up to 300 times[17,25] or 50 to 100 times[14] and a surface area of 600–800 $m^2 g^{-1}$.[22]

To further support the aforementioned observations on the degree of exfoliation, the samples were characterized by XRD. As shown in Figure 1. It can be seen that the flake graphite undergo several graphitic structural changes upon oxidation and

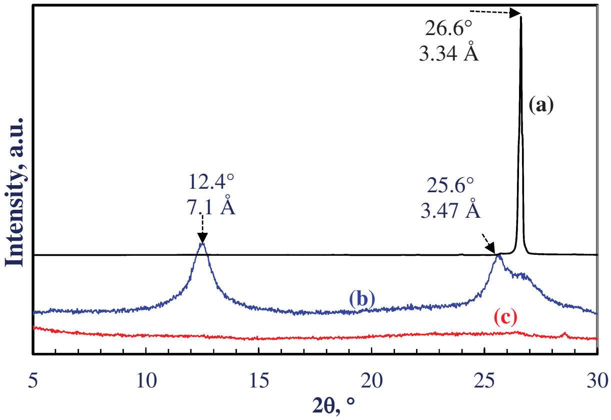

Figure 1.
XRD patterns of natural flake graphite, (a), graphite oxide, (b), and graphite nanosheets (GNS), (c).

thermal reduction, in particular the increasing of the c-axis spacing. Flake graphite possesses two strong peaks at 26.6° and 55° and graphite oxide two weak peaks at 12.5° and 26°. The peak at 12.5° results from the increasing of the layer spacing during oxidation and is corresponding to d-spacing of 0.71 nm, whereas the native peak at 26.6° which is present in the flake graphite weakens corresponding to the lower distance in the graphitic crystal lattice of 0.33 nm. The second step in the exfoliation process involves rapid thermal heating to 1000 °C at a rate of 2000 °/min. This rapid heating leads to i) evaporation of water molecules that are strongly adsorbed and intercalated within the graphitic gallery, ii) removal of some of the oxygen containing groups in the form of CO_2. The pressure generated because of that result in complete separation of the graphene sheets of the oxidized graphite sample which is more liable to exfoliation than the pristine graphite due to the weaker van de Walls in the oxidized sample due to the large layer spacing. Hence, absence of any significant diffraction peaks in the XRD pattern for the GNS confirms the complete exfoliation of graphite to nano-graphite.

The morphological features of the resulting GNS were investigated by SEM and images are shown in Figure 2. The collapsed layers are observed either as loose sheets or are irregularly arranged forming a network structure like folded paper with pores of different sizes that indicates the extremely low density of the GNS powder. The estimated average

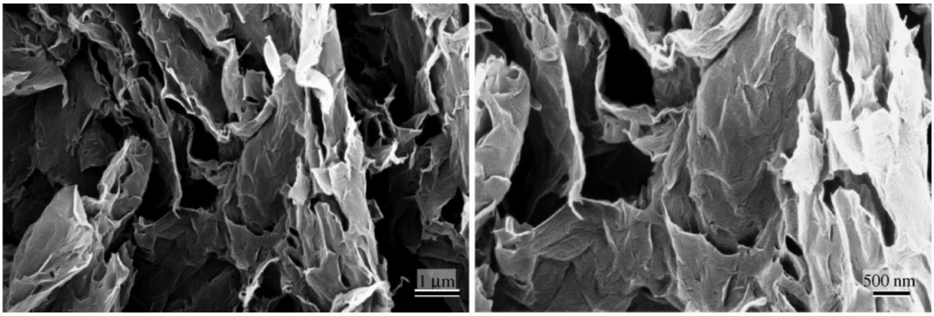

Figure 2.
Scanning electron micrographs of GNS.

diameter of the obtained single graphite nano sheets is about 5 μm. The thickness of the nano sheets is in the nanometer scale and ranged from 100 to 400 nm. Several groups reported similar sheet sizes of 1–20 μm and sheet thicknesses ranged from 50–100 nm.[9–11,14,26,27] The structure and size of a GNS particle are strongly depending on the degree of exfoliation which is primarily affected by the exfoliation time and temperature. It is observed that a higher temperature leads to smaller particle sizes[6] and further sonication could also reduce the GNS particle size.[27]

Characterization of GNS/Melamine Composites

A series of GNS filled melamine formaldehyde resin composites were prepared and their morphological, thermal and electrical behavior were analyzed. Samples of unfilled melamine formaldehyde resins and others filled with activated carbon were made and used for comparison purpose.

Microstructure of GNS/Melamine Composites

To examine the interfacial interaction between the GNS and melamine resin, fractured sections of the monoliths were investigated by SEM, and the corresponding micrographs are shown in Figure 3. To some extent, these cross-sectional SEM micrographs reflect the dispersion of GNS in the melamine-formaldehyde resin. At very low GNS content (0.1 wt.%), composites reveal a smooth and less fractured surface (Figure 3a), suggesting homogeneity of thermosetting material. It is notable that the increase in GNS content shows the existence of crumpled graphitic sheets which are finely distributed in the matrix,

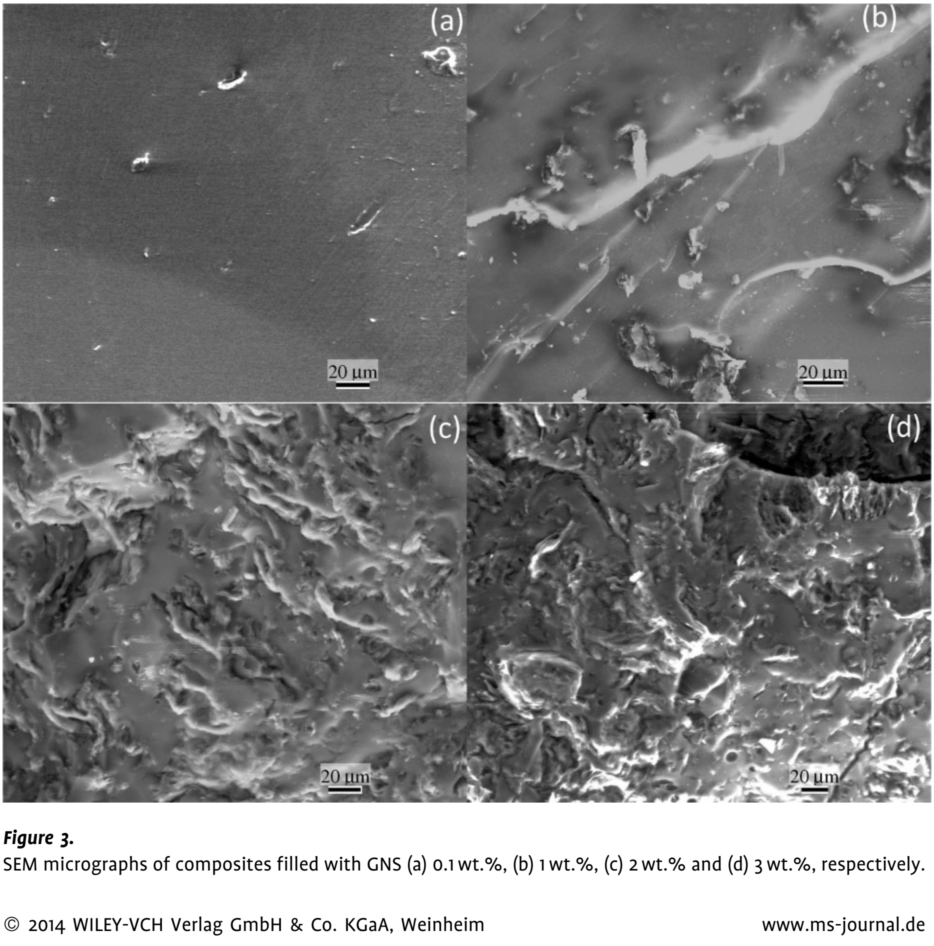

Figure 3.
SEM micrographs of composites filled with GNS (a) 0.1 wt.%, (b) 1 wt.%, (c) 2 wt.% and (d) 3 wt.%, respectively.

confirming their presence in the melamine matrix. The possible interactions between the carboxyl and hydroxyl groups on the edge of GNS sheets and amino-resin may have facilitated the GNS dispersion in the final resin composites. The fracture surfaces of GNS/melamine composites (Figure 3b–d) are rough and consist of many small facets, elucidating that the nano graphite inhibits fracture of the composites and thus results in a rougher fracture surface. Hence, higher loading of GNS sheets dramatically changes the morphology of resin composites, primarily due to their high content and large surface area that could generate a 2-dimensional hindrance and toughening effect on the matrix, which resulted in a much coarser fracture surface.

Thermal Stability

MF undergoes several degradation steps in the range 50–900 °C. As shown in Figure 4, the thermal decomposition thermogram for pure MF consist of several degradation steps: a slow weight loss step between 50–150 °C; second slow weight loss step between 150–364 °C; a rapid weight loss between 364–400 °C; another slow weight loss region between 400–660 °C, and a final degradation step above 660 °C. These transition steps are attributed to water evaporation; release of formaldehyde and amine, release of formadelhdye, amine, carbon dioxide, and ammonia; degradation of melamine; and the extensive degradation of MF and the formation of HCN, CO, and CO_2, respectively.[26,28]

In general, the composite samples with 1 and 2 wt.% GNS is more thermally stable than pure MF as it maintain higher residual mass than pure MF over the entire temperature range. Nonetheless, the most significant effect of the addition of GNS is on the rapid thermal decomposition step. This can be clearly demonstrated by the increase in the onset temperature for the rapid degradation step from 364 from MF to 374 with 1% GNS and to 380 with 3% GNS as shown in the bottom inset of Figure 4. Moreover, GNS seems also to reduce the release of water and formaldehyde as shown by the lower weight loss associated with the composite samples compared to pure MF in the range of 50–360 C. At temperatures above 800 °C a higher amount of thermally stable char is obtained when GNS was incorporated. This amount of stable char increases with GNS loading, see the upper inset in Figure 4.

Electrical Conductivity

The most important effect of GNS is on the electrical properties of MF. Electrically conductive MF composite is obtained using

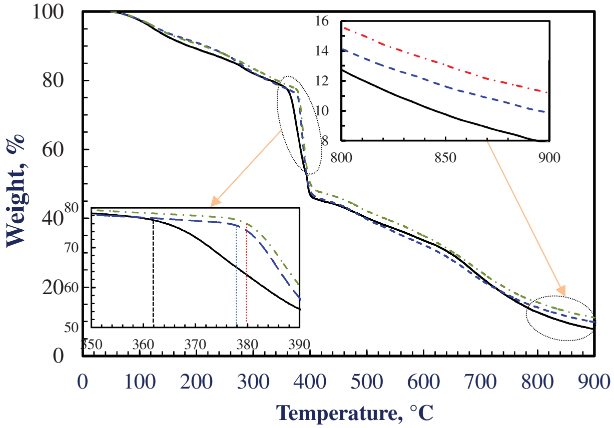

Figure 4.
Thermogravimetric analysis of melamine/GNS composites 0.0 wt.% (—), 1.0 wt.% (- - -), and 3 wt.% (—·—·—), respectively.

a low GNS loading. Figure 5 provides the average resistance value for pure and composite samples with various GNS loadings. The conductivity percolation threshold is achieved at GNS loading about 1.3 wt.% (0.89 vol.%). According to the classical percolation theory, the percolation threshold corresponds to the onset of the transition from an insulator to an electrical semiconductor.[29] The percolation threshold is a measure of the filler aspect ratio, a. Different theoretical models predict the percolation threshold as a function of the filler aspect ratio, a. For example, Celzard Model[30] predicts percolation loading, φ_C, between $1 - \exp\left(-\frac{3.6}{\pi a}\right)$ and $1 - \exp\left(-\frac{5.6}{\pi a}\right)$. On the other hand, Lu and Mai Model[31] predicts $\varphi_C = \frac{2.154}{a}$. For MF composites with $\varphi_C = 0.0089$, the predicted aspect ratio based on Celzard model is between 128 and 199 while Lu and Mai model suggests an aspect ratio of 242. Assuming a lateral dimension of GNS of 2 μm as implied by the SEM images in Figure 2, the thickness of GNS would range between 8 and 16 nm based on the predicted aspect ratio.

The percolation threshold also depends further on the geometry of the conducting fillers. Fillers with elongated or expanded geometry such as fibers or sheets possess lower percolation thresholds because they can better form conducting networks in a polymer matrix. Therefore it is obviously that GNS composites require a much lower percolation threshold than activated carbon or graphite powder composites. In the present study, we observed significantly lower percolation threshold for melamine composites in comparison with common thermoplastics such as polystyrene (6–7 wt.%)[12,27] and PMMA (5 wt.%).[9]

As GNS increases above φ_C, the electrical resistance rapidly decreases from 4.3×10^{11} Ω for pure MF to 2.5×10^{4} Ω at 2 wt.% and reduces further to 3.1×10^{3} Ω at 3 wt.%.

The significant decrease in the resistance of MF-GNS composites is due to the homogenous dispersion of GNS and formation to a conducting network at a low loading of GNS.

Conclusion

GNS with BET surface area of 600 m^2/g and a specific volume of 300 ml/g were prepared by thermal exfoliation of graphite oxide at 900 °C. The average lateral size of GNS is about 5 μm and the thickness of 100–400 nm as observed from SEM images GNS/Melamine-formaldehyde nanocomposites were produced by an in situ polymerization. The good dispersion of GNS and its incorporation into the melamine-formaldehyde matrix was confirmed by SEM. The

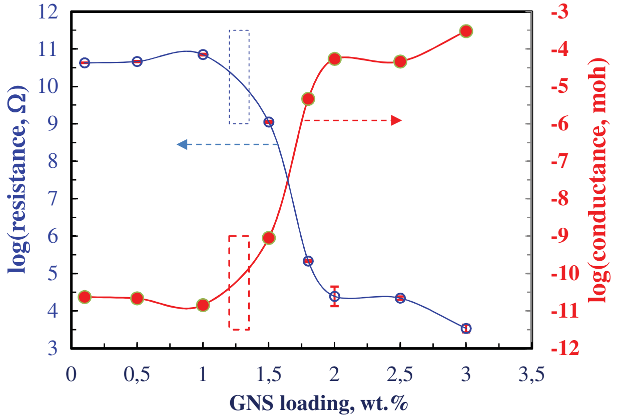

Figure 5.
Electrical Resistance of MF composite with different loading of GNS.

resulting GNS/melamine composites showed improved electrical conductivity over the unfilled MF resins. Moreover, a percolation threshold below 0.9 vol.% of GNS was attained. Moreover, the produced composite exhibits improved thermal stability as indicated by the shift in the onset of the rapid degradation step. Hence, the incorporation of GNS into melamine-formaldehyde resins via in-situ polymerization method is a viable approach to fabricate electrically conductive thermoset resins.

[1] S. Bourdo, T. Viswanathan, *Carbon* **2005**, *43*, 2983.

[2] V. Causin, et al., *European Polymer Journal* **2006**, *42*, 3161.

[3] V. Mironov, et al., *Polymer testing* **2007**, *26*, 547.

[4] Q. Yin, et al., *Journal of power sources* **2007**, *165*, 717.

[5] F. M. Uhl, et al., *Polymer Degradation and Stability* **2005**, *89*, 70.

[6] M. Inagaki, F. Kang, M. Toyoda, *Chem. Phys. Carbon* **2004**, *29*, 1.

[7] G. Chen, et al., *European Polymer Journal* **2003**, *39*, 2329.

[8] H.-B. Zhang, et al., *Polymer* **2010**, *51*, 1191.

[9] W. Zheng, S.-C. Wong, *Composites Science and Technology* **2003**, *63*, 225.

[10] K. Kalaitzidou, H. Fukushima, L. T. Drzal, *Composites Part A: Applied Science and Manufacturing* **2007**, *38*, 1675.

[11] K. Kalaitzidou, H. Fukushima, L. T. Drzal, *Composites Science and Technology* **2007**, *67*, 2045.

[12] G. Chen, et al., *Polymer* **2003**, *44*, 1781.

[13] P. Xiao, M. Xiao, K. Gong, *Polymer* **2001**, *42*, 4813.

[14] G. Zheng, et al., *Carbon* **2004**, *42*, 2839.

[15] L. Du, S. C. Jana, *Journal of Power Sources* **2007**, *172*, 734.

[16] J. Li, J.-K. Kim, M. Lung Sham, *Scripta Materialia* **2005**, *53*, 235.

[17] Y. Zhao, et al., *Composites science and technology* **2007**, *67*, 2528.

[18] X. S. Du, M. Xiao, Y. Z. Meng, *European Polymer Journal* **2004**, *40*, 1489.

[19] H. Wang, H. Zhang, G. Chen, *Composites Part A: Applied Science and Manufacturing* **2007**, *38*, 2116.

[20] Q. Yin, et al., *Journal of Power Sources* **2008**, *175*, 861.

[21] X. Zhang, et al., *Materials Chemistry and Physics* **2008**, *111*, 368.

[22] T. Ramanathan, et al., *Nature Nanotechnology* **2008**, *3*, 327.

[23] M. J. McAllister, et al., *Chemistry of Materials* **2007**, *19*, 4396.

[24] D. J. Merline, S. Vukusic, A. A. Abdala, *Polym. Journal* **2013**, *45*, 413.

[25] B. Debelak, K. Lafdi, *Carbon* **2007**, *45*, 1727.

[26] C. Schwarzinger, et al., *International Journal of Polymer Analysis and Characterization* **2007**, *12*, 143.

[27] G. Chen, et al., *Carbon* **2003**, *41*, 619.

[28] C. Devallencourt, et al., *Thermochimica acta* **1995**, *259*, 143.

[29] D. Stauffer, A. Aharony, Introduction to percolation theory. **1994**, CRC press.

[30] A. Celzard, et al., *Physical Review-Section B-Condensed Matter* **1996**, *53*, 6209.

[31] C. Lu, Y.-W. Mai, *Physical review letters* **2005**, *95*, 088303.